ECLÉTICA QUÍMICA

Eclet. Quim. 50 | e-1594, 2025

Original Article

https://doi.org/10.26850/1678-4618.eq.v50.2025.e1594

Molecular modeling and pharmacokinetics studies of sulfamidophosphonate derivatives as potential candidate against *Staphylococcus aureus*

Abimbola Modupe **Olatunde**[1], Kehinde Gabriel **Obiyenwa**[2], Tofunmi Emmanuel **Oladuji**[3], Dayo Felix **Latona**[4], Abel Kolawole **Oyebamiji**[5,6], Nathaniel Oladoye **Olatunji**[3], Banjo **Semire**[2,3+]

Abstract

In silico methods were used in this paper to assess the anti-bacterial activity of Sulfamidophosphonate derivatives against *Staphylococcus aureus* proteins (1XSD and 4WK3) using molecular docking and ADMET analysis. The results showed that binding affinity (ΔG kJ/mol) ranged from –4.1(NAM) to –7.1 kJ/mol (NAL) for 1XSD, and –5.0 (NAE) to –6.7 kJ/mol (NAM) for 4WK3. Therefore, compounds NAH, NAL, NAN, NAI, NAJ, NAK, 5AD and NAM could be more desirable as inhibitors than Penicillin (–6.0 kJ/mol for 1XSD and –5.4 kJ/mol for 4WK3) in the treatment of *Staphylococcus aureus*; but ADMET profile revealed that compounds NAF, NAI, NAK NAN and 5AC present attractive pharmacokinetic properties. In this study, compounds NAH, NAL, NAI and NAJ exhibited stronger affinities than the standard (penicillin) against BlaI repressor in complex with DNA (PDB ID: 1XSD) suggesting better inhibitory potential than the standard drug.

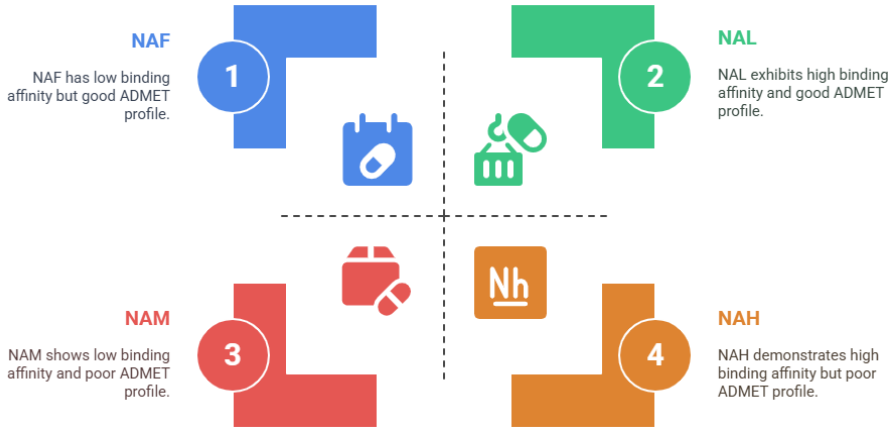

Article History

Received September 02, 2024
Accepted December 19, 2024
Published June 26, 2025

Keywords

1. phytochemicals;
2. *bacteria*;
3. interactions;
4. ADMET.

Section Editors

Assis Vicente Benedetti

Highlights

- The antibacterial activity of sulfamidophosphonate derivatives was evaluated.
- Descriptors found from optimized sulfamidophosphonate derivatives were identified.
- Nonbonding interactions between drugs and the studied targets were observed.

[1]University of Ibadan, Department of Chemistry, Ibadan, Nigeria. [2]Federal University of Lokoja, Department of Chemistry, Lokoja, Nigeria. [3]Ladoke Akintola University of Technology, Department of Pure and Applied Chemistry, Ogbomoso, Nigeria. [4]Osun State University, Department of Pure and Applied Chemistry, Osogbo, Nigeria. [5]University of Ilesa, Department of Industrial Chemistry, Ilesa, Nigeria. [6]University of Ilesa, Good Health and Wellbeing Research Clusters, Ilesa, Nigeria. **+Corresponding author:** Banjo Semire, **Phone:** +2348038269809, **Email address:** bsemire@lautech.edu.ng

1. Introduction

Bacterial diseases such as tuberculosis, anthrax, pneumonia and osteomyelitis, among others, are deadly and have a significant impact on public health. *Staphylococcus aureus* is both a commensal bacterium and a human pathogen. About 30% of the human population is colonized with *S. aureus* (Wertheim *et al.,* 2005). In the early 1930s, doctors began to employ a more efficient test to determine the presence of an S. *aureus* infection by means of coagulase testing, which helped to detect the enzyme produced by the bacterium. Before the 1940s, *S. aureus* infections were deadly in most patients until the discovery of penicillin. However, the Meca gene carried by Methicillin-resistant *Staphylococcus Aureus* (MRSA) encodes the protein PBP-2a (penicillin-binding protein 2a) marked the outbreaks of the resistant strain of this bacterium family (Orent, 2006). The PBP-2a is a penicillin-binding protein (PBP), or an essential bacterial cell wall enzyme that catalyzes the production of the peptidoglycan in the bacterial cell wall. PBP-2A has a lower affinity to bind to beta-lactams (and other penicillin-derived antibiotics) when compared to other PBPS. The PBP-2A continues to catalyze the synthesis of the bacterial cell wall even in the presence of many antibiotics (Rasigade, 2014).

The chemistry of heterocyclic molecules plays a huge role in the development of effective drugs for bacterial, fungal and viral diseases. Heterocyclic compounds are the most important organic compounds that present great interest in medicinal chemistry (Arora *et al.*, 2012; Winum *et al.*, 2006*).* Sulfonamide derivatives, a class of heterocyclic compounds in which many this class compounds have been reported to show biological activities such as anti-mycobacterial, anticonvulsant, anti-hypoglycemic, anticancer, and enzyme inhibition (Farhan *et al.*, 2018; Hu *et al.*, 2008; Supuran, 2017; Zhao *et al.*, 2019). Sulfonamide derivatives are attractive due to their diverse biological targets and practical therapeutic ability with minimal side effects (Hu *et al.*, 2008; Ratchanok, 2021).

Presently, there have been a remarkable advance in the development of new potent antibiotics for combating antimicrobial resistance (Bazine *et al.*, 2020a; Masters *et al.,* 2003); however, the microorganisms are getting resistant to the existing antibiotic classes by mutation of membrane permeability and spore formation to the drugs (Forgacs *et al.,* 2009) thereby adapting themselves to withstand the potency of the drug. This has led to continuous research on drug development and discovery to produce new drugs that can fight the resistance caused by *Staphylococcus Aureus*. In recent times, Sulfamidophosphonate, a sulfonamide and cyclosulfamide derivative, have been a focus of chemical and biological researchers for the development of new drugs, due to its wide range of biological and physical properties (Krátký *et al.,* 2012; Waring *et al.*, 2015). In this study, computational methods, including molecular docking and ADMET profiling to evaluate antibacterial activities of some selected Sulfamidophosphonate derivatives based on the work of Bazine *et al.* (2020b). These compounds are 1-(1,1-dioxo-1λ^6,2,5-thiadiazolidin-2-yl)(2-oxo-1,2,3,4-tetrahydroquinolin-3-yl)(1,1-diethoxyphosphonate (**5AD**), 1,1-(3-methylphenyl-sulfonamidyl)(6-methyl-3,4-dihydroquinolin-2(1*H*)-onyl)methyl)(1,1-diethoxy)phosphonate (**NAI**), 1,1-(3-methylphenyl-sulfonamidyl)(3,4-dihydroquinolin-2(1*H*)-onyl)methyl)(1,1-diethoxy)phosphonate (**NAH**), 1,1-(phenyl-sulfonamidyl)(6-methyl-3,4-dihydroquinolin-2(1*H*)-onyl)methyl)(1,1-diethoxy)phosphonate (**NAJ**), 1,1-(2-methylphenyl-sulfonamidyl)(3,4-dihydroquinolin-2(1*H*)-onyl)methyl)(1,1-diethoxy)phosphonate (**NAK**), 1,1-(3-methylphenyl)-sulfonamidyl)(2-methyl-3,4-dihydroquinolin-2(1*H*)-onyl)methyl)(1,1-diethoxy)phosphonate (**NAL**), 1,1-(3-chlorophenyl)-sulfonamidyl)(2-methyl-3,4-dihydroquinolin-2(1*H*)-onyl)methyl)(1,1-diethoxy)phosphonate (**NAM**), and 1,1-(2-hydroxylphenyl)-sulfonamidyl)(2-methyl-3,4-dihydroquinolin-2(1*H*)-onyl)methyl)(1,1-diethoxy)phosphonate (**NAN**).

2. Details of research methods

2.1. Geometry optimization of the ligands

The conformer search was carried out on each sulfamidophosphonate using the DFT method to find the conformer with the lowest energy for each compound, which was then taken as the equilibrium geometry structure of the compound. The equilibrium optimization was performed on the ligands (**Fig. 1**) with DFT in correlation with Becke's three-parameter hybrid functional with a correlation of Lee, Yang and Parr (B3LYP) (Becke, 1993; Hehre *et al.,* 1988; Parr *et al.*, 1999; Yang *et al.*, 2005; Lee *et al.*, 1988) with 6-31G(d,p) basis set. Quantum chemical reactivity descriptors of the sulfamidophosphonates such as frontier orbital energies, which are the highest occupied molecular orbital energy (E_{HOMO}), the lowest unoccupied molecular orbital energy (E_{LUMO}) and band energy gap ($E_{(HOMO-LUMO)}$); chemical hardness ($\eta = \frac{E_{HOMO}-E_{LUMO}}{2}$); chemical softness ($\sigma = \frac{1}{2\eta}$); chemical potential ($\mu = \left(\frac{E_{HOMO}+E_{LUMO}}{2}\right)$; global electrophilicity ($\omega = \frac{\mu^2}{2\eta} = \frac{(IP+EA)^2}{4(IP-EA)}$); electron donating power ($\omega^- = \frac{(3IP+EA)^2}{16(IP-EA)}$) and electron accepting power ($\omega^+ = \frac{(IP+3EA)^2}{16(IP-EA)}$) were estimated form the optimized structures (Flores-Holguín *et al.*, 2019; Manzanilla and Robles, 2020; Ramírez-Martínez *et at.*, 2023).

2.2. Molecular docking procedures

The optimized ligands were docked into the receptors by using Autodock Tool 1.5.6., AutoDock Vina 1.1.2, Edupymol version 1.7.4.4 and Discovery studio. The receptors/proteins were cleaned up and repaired with Discovery Studio software, and Edupymol was used to visualize the docking results as described (Adegbola *et al.*, 2021a; Adepoju *et al.*, 2022; Oyebamiji *et al.*, 2021). The binding pocket of the protein, as determined in the 3D structure using Discovery Studio and the Autodock tool, was used to prepare the protein. Polar hydrogens were added to the protein, followed by Kolleman charges, before setting the grid box. Using Auto Grid, the grid box center (x = –5.252, y = 9.613, z = 36.518) and size (x = 58, y = 52, z = 66) for BlaI repressor in complex with DNA (**PDB ID: 1XSD**), and (center: x = 0.043, y = 2.734, z = 85.68) and (size: x = 48, y = 40, z = 40) for **4WK3** receptor were set. The receptor and ligand were then saved as PDBQT files. The Docking simulations were then performed using Autodock Vina (Trott *et al.,* 2010) for the calculations of binding affinity, as well as studying non-bonding interactions (hydrophobic interactions) and hydrogen bonding between the ligand and proteins, which were visualized using Discovery Studio 2019.

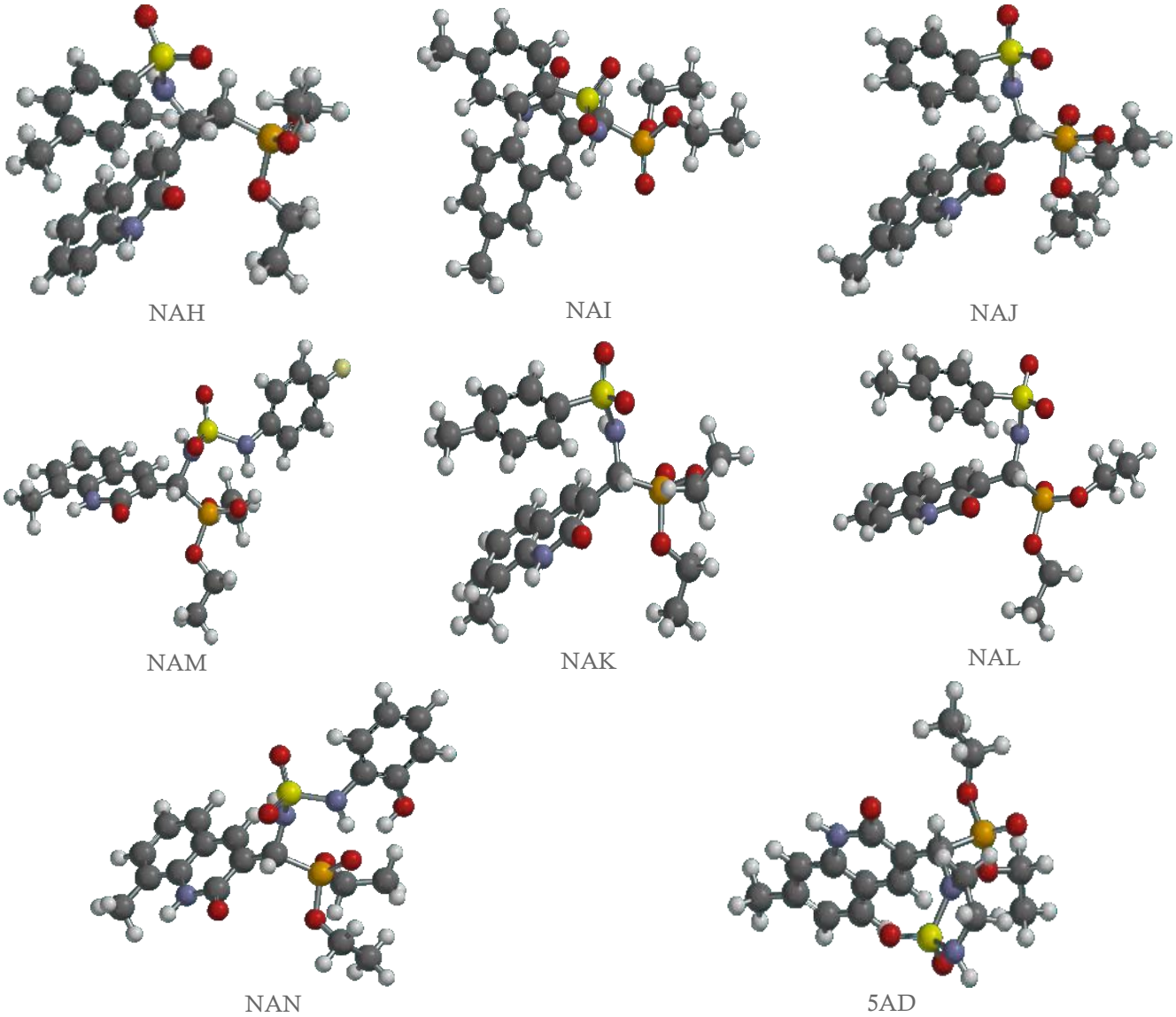

Figure 1. Optimized structures of studied sulfamidophosphonates.
Source: Elaborated by the authors.

2.3. ADME/pharmacokinetic predictions

The smiles of optimized structures of the studied ligands were used for physicochemical and ADMET profiles to assess the qualitative pharmacokinetics properties via; absorption, distribution, metabolism, excretion and toxicity by using ADMET Predictor (http://biosig.unimelb.edu.au/pkcsm/prediction). These early assessments of pharmacokinetic and toxic properties are essential step in drug discovery, although the process of drug discovery and development is a very complex, lengthy and cost-intensive; drug development failures have been attributed to poor pharmacokinetics and bioavailability (Adegbola *et al.*, 2021b; Daina and Zoete, 2016). Therefore, ADMET properties play a crucial role in every stage of drug discovery and development, aiming to reduce likely challenges associated with clinical trial treatments (Darvas *et al.,* 2002).

3. Results and discussion

3.1. Molecular quantum reactivity descriptors

The frontier orbital (the HOMO and LUMO) energies are very essential to the molecular stability and responses to the surrounding molecules, where HOMO and LUMO represent the highest occupied molecular orbital and the lowest unoccupied molecular orbital, respectively. The high HOMO energy (or low ionization energy, IP) typifies the enhancement of a ligand to donate electrons to the neighboring molecule. Lower LUMO energy, on the other hand (or high electron affinity, EA), represents a ligand's ability to accept electrons from the neighboring compounds (Oyebamiji and Semire, 2016). The lower IP values revealed that NAH (4.05 eV), 5AD (5.47 eV), and NAN (5.75 eV) should be able to donate electrons readily to the

surrounding molecule than Penicillin (9.61 eV) and Sulfamethoxazole (5.93 eV) (Oyeneyin, 2023). Also, all the compounds, especially NAL, NAH, 5AD, NAM, and NAN, should have enhanced electron-accepting tendency from the neighboring molecule (Table 1). Low polarizability, low reactivity, stronger stabilization and interactions between a molecule and its receptor favor molecules with a larger energy gap (Eg), whereas a smaller energy gap favors high reactivity, high polarizability, weaker stabilization and interactions of a molecule with neighboring compound. Therefore, higher values, Eg, η and σ, showed that penicillin and Sulfamethoxazole are more stable, which may support strong interactions, although NAJ, NAI, NAK and NAM may also display strong interactions (Thanikaivelan *et al.,* 2020).

The chemical potential (μ) showed that all the sulfamidophosphonate compounds are more likely to interact strongly through electrostatic interactions with the receptor than the standard drugs (penicillin and Sulfamethoxazole). The difference between electron-donating ability (ω–) and electron-accepting ability (ω+) is |Δω|, which measures the total responsiveness of a molecule to its surroundings. Higher values typify a strong response leading to strong interactions between the molecule and its surroundings (Asibor *et al.*, 2024). Therefore, NAL, NAM, NAK, NAJ, and 5AD are likely disposed of stronger interactions with the receptor than penicillin and Sulfamethoxazole.

Table 1. Quantum chemical descriptors of sulfamidophosphonates using B3LYP/6-31G**.

	IP	EA	Eg	η	σ	μ	ω	ω-	ω+	$\lvert\Delta\omega\rvert = (\omega^{+} - \omega^{-})$
NAH	4.05	2.68	1.37	0.685	0.730	–3.365	8.265	10.033	6.668	3.365
NAI	6.26	1.81	4.45	2.225	0.225	–4.035	3.659	5.954	1.919	4.035
NAJ	6.11	1.55	4.56	2.280	0.219	–3.830	3.217	5.417	1.587	3.830
NAK	6.33	1.80	4.53	2.265	0.221	–4.065	3.648	5.963	1.898	4.065
NAL	6.47	4.01	2.46	1.230	0.407	–5.240	11.162	13.935	8.695	5.240
NAM	6.22	2.03	4.19	2.095	0.239	–4.125	4.061	6.385	2.260	4.125
NAN	5.75	2.03	3.72	1.860	0.269	–3.890	4.068	6.245	2.355	3.890
5AD	5.47	2.54	2.93	1.465	0.341	–4.005	5.474	7.660	3.655	4.005
Penicillin	9.61	–3.34	12.95	6.475	0.077	–3.135	0.759	3.136	0.001	3.135
Sulfamethoxazole	5.93	0.51	5.42	2.710	0.185	–3.220	1.913	3.862	0.642	3.220

Source: Elaborated by the authors.

3.2. Docking orientation and binding affinity

BlaI is a repressor, as well as a beta-lactamase that is responsible for penicillin resistance in *Staphylococcus aureus* and essential for *Staphylococcus aureus* reproduction. The BlaI repressor in complex with DNA (**PDB ID: 1XSD**) was docked with sulfamidophosphonate derivatives. Results were presented in **Table 2** and **Fig. 2**. The binding affinities for all the studied ligands with **1XSD** ranged from –17.2 (NAM) to –29.7 (NAL) kJ/mol, these inferred that inhibitory constants (Ki) of the drugs fall between 6.21 μmol/L to 984.0 μmol/L as compared to –25.1 kJ/mol for penicillin, used as standard (**Table 2**). The H-bond distances between amino acid residues in the binding purse and ligands ranged from 1.9 to 3.50 Å. They exhibited other non-bonding interactions with **1XSD** receptor (**Fig. 2**). Compound/ligand **NAL** with the highest binding affinity (–29.7 kJ/mol) is hydrogen bonded with ARG'60, TYR'69, ARG'46, ARG' 46 and THR'50 and showed interactions with ALA'27, TYR'67, TYR'69, ARG'46, THR'50 and ARG'60. **NAN** with the binding affinity of –23.8 kJ/mol displayed H-bond interactions with ARG'60 and TYR 69, and hydrophobic interactions with ARG 46, TYR'69, LYS'54, ALA'27, ARG'60 and THR'50. Also, **NAI** and **NAK** with binding affinities of –28.5 and –25.1 kJ/mol, respectively, showed only hydrophobic interactions with PHE'86, LEU'98, PHE'102, TRP'13 and ALA'83 for **NAI**, and LYS'69, ALA'83, PHE'86 for **NAK**. Ligand **NAJ** with a binding affinity of –28.0 kJ/mol hydrophobically interacted with LYS'54 ARG'60 ARG'46 TYR'69, and THR'50, as well as H-bonding with ARG'26 and ARG'60**.** Also, **NAH** presented H-Bonding with ARG'26 and ARG'60' and hydrophobic interactions with ARG'60, TYR'67, ILE'66, and LYS'43.

Furthermore, **5AD** with a binding affinity of -26.4 kJ/mol is hydrogen-bonded with **TYR'59 ARG'46** and **TYR'69** and shows hydrophobic interactions with **ARG'60 TYR'69** and **ARG'46**, while **NAM** with a binding affinity of –17.2 kJ/mol displayed hydrophobic interactions with **LYS'43 ARG'46** and **TYR'67**. Penicillin, which was used as the standard drug, has a binding energy of –25.1 kJ/mol, interacting hydrophobically with **ALA'83 ASN'17** and **PHE'86**. The ionization energy (IP = $-E_{HOMO}$) and electron affinity (EA = $-E_{LUMO}$) estimated from the DFT calculations showed that NAL has highest values for both IP (6.47 eV) and EA (4.01 eV) which led to lower energy gap; thus, supported quick electrons transition and donation to the receptor than other compounds. Therefore, NAL, NAH, NAI and NAJ exhibited the most significant inhibitory potential against **1XSD** when compared with the standard drug (penicillin).

Table 2. Binding affinity and non-bonding interactions of **1XSD** and **4WK3 receptors** with ligands.

Ligand	1XSD	4WK3
	Binding Affinity ΔG (kJ/mol)	Binding Affinity ΔG (kJ/mol)
NAH	−26.4	−24.3
NAI	−27.6	−24.7
NAJ	−28.5	−25.1
NAK	−26.8	−25.5
NAL	−27.2	−24.3
NAM	−25.9	−28.0
NAN	−23.8	−28.0
5AD	−24.3	−23.0
Penicillin	−26.4	−22.6
Sulfamethoxazole	−23.4	−22.6

Source: Elaborated by the authors.

https://doi.org/10.26850/1678-4618.eq.v50.2025.e1594

2D Structure | 3D Structure

1XSD + NAH

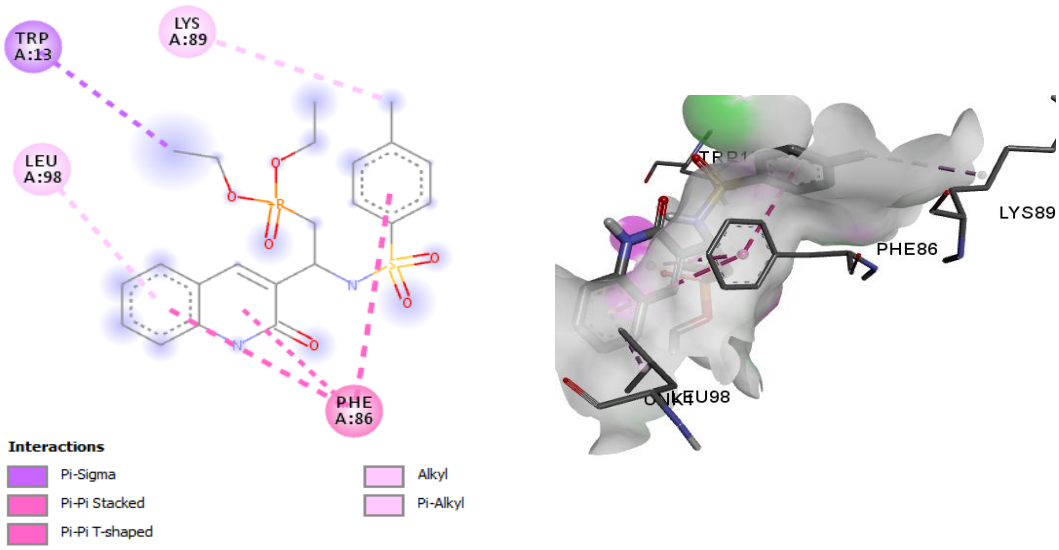

1XSD + NAI

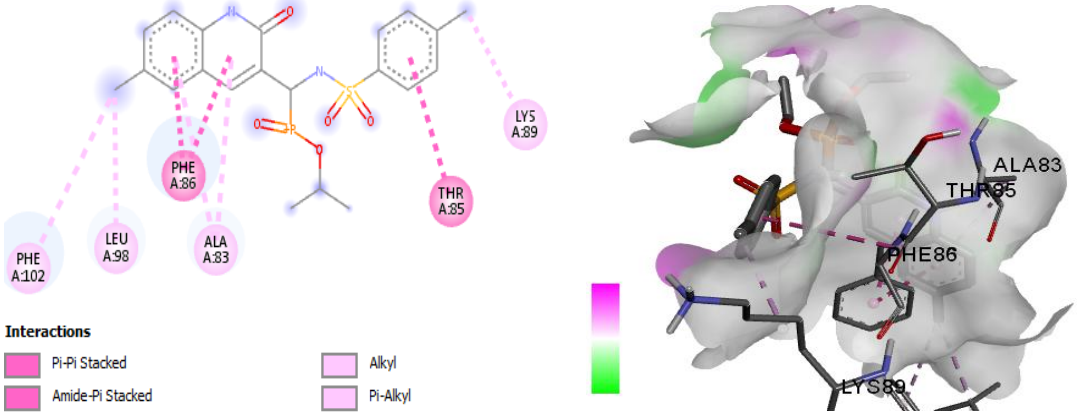

1XSD + NAJ

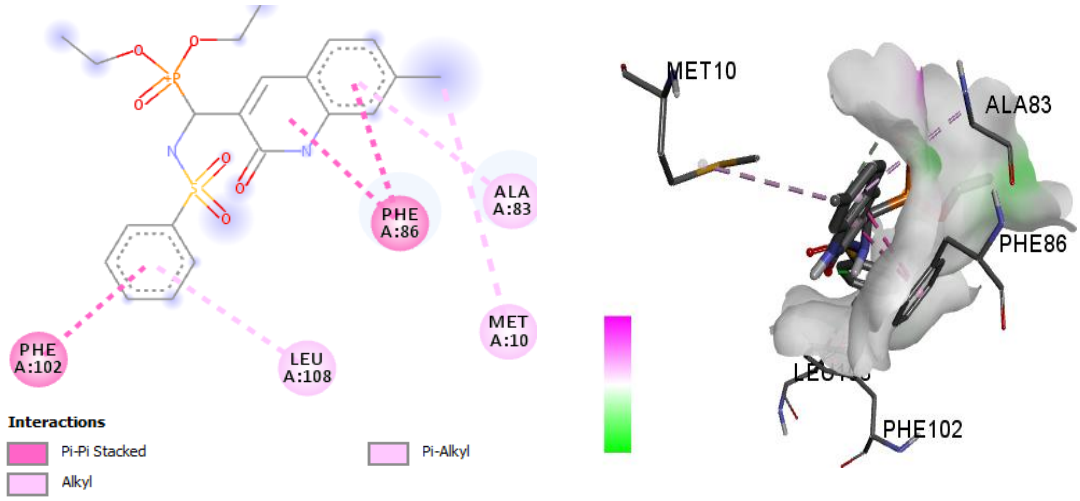

https://doi.org/10.26850/1678-4618.eq.v50.2025.e1594

1XSD + NAK

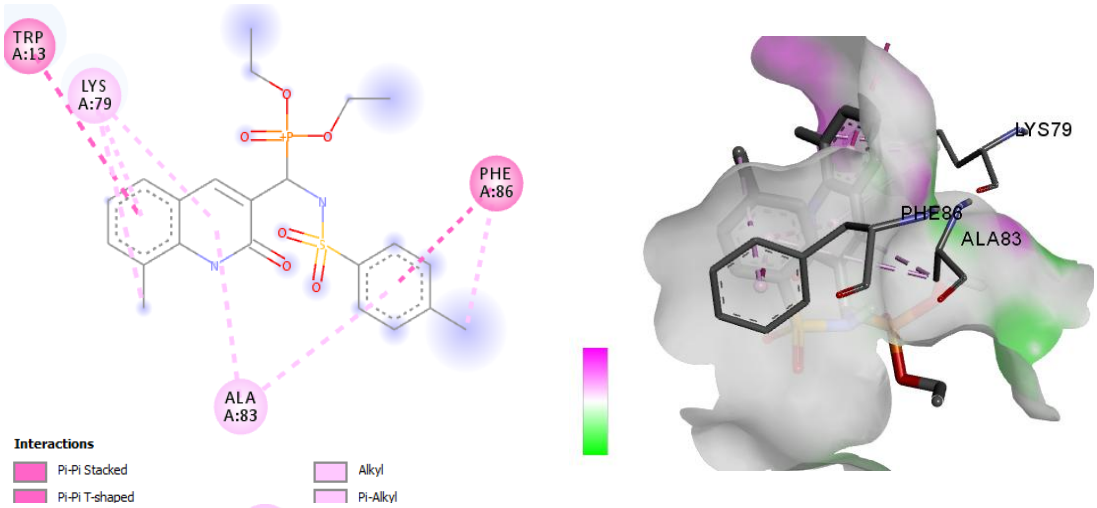

1XSD + NAL

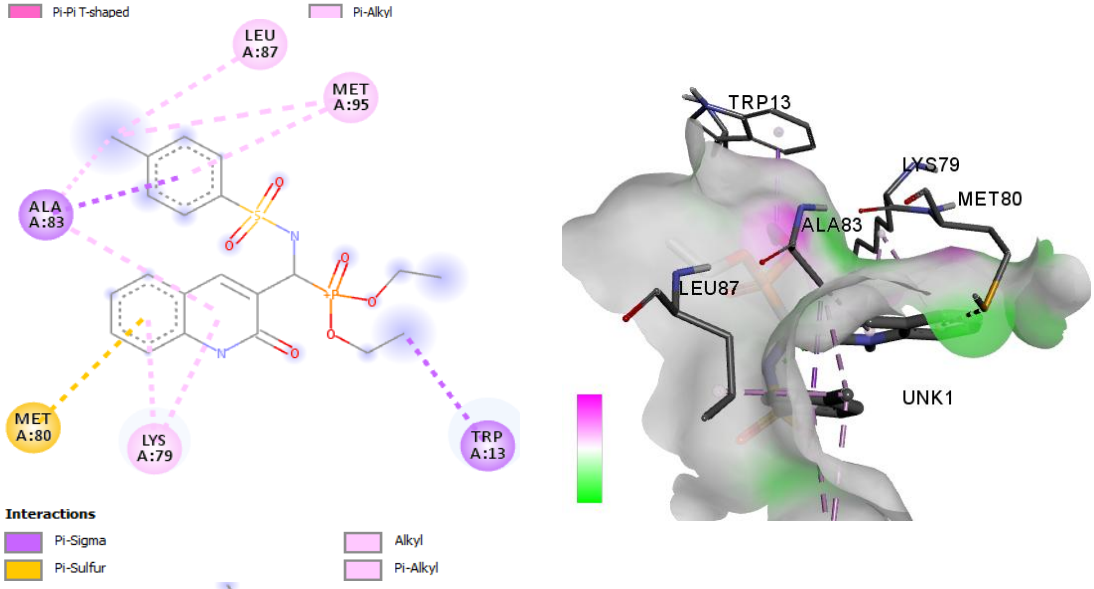

1XSD +NAM

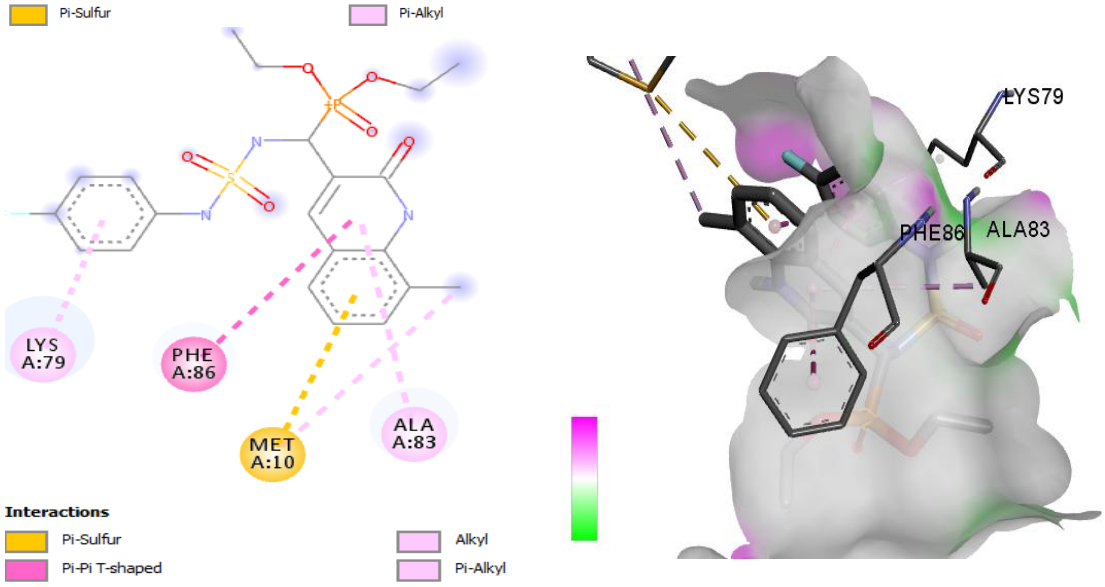

https://doi.org/10.26850/1678-4618.eq.v50.2025.e1594

1XSD +NAN

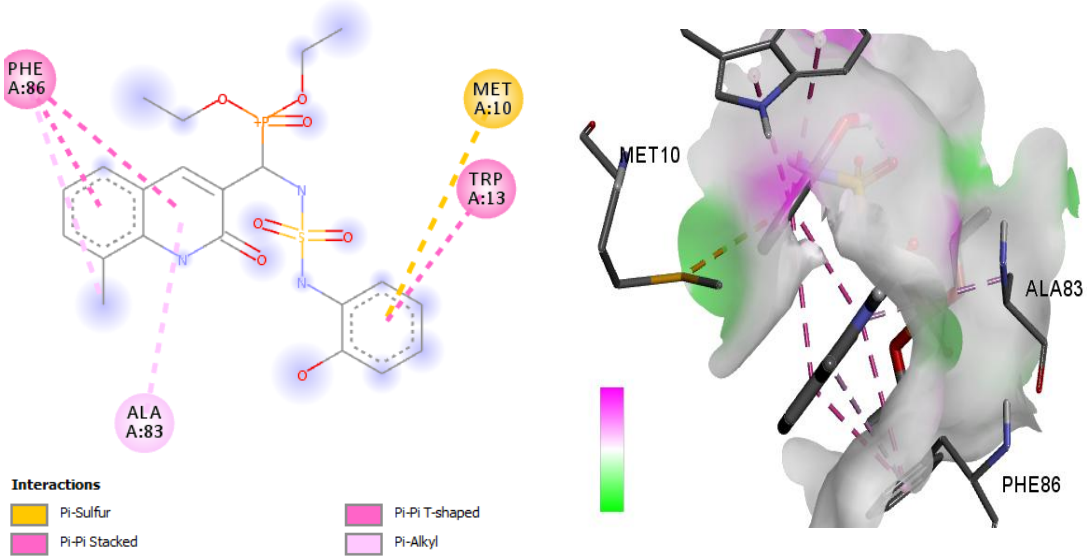

1XSD+ 5AD

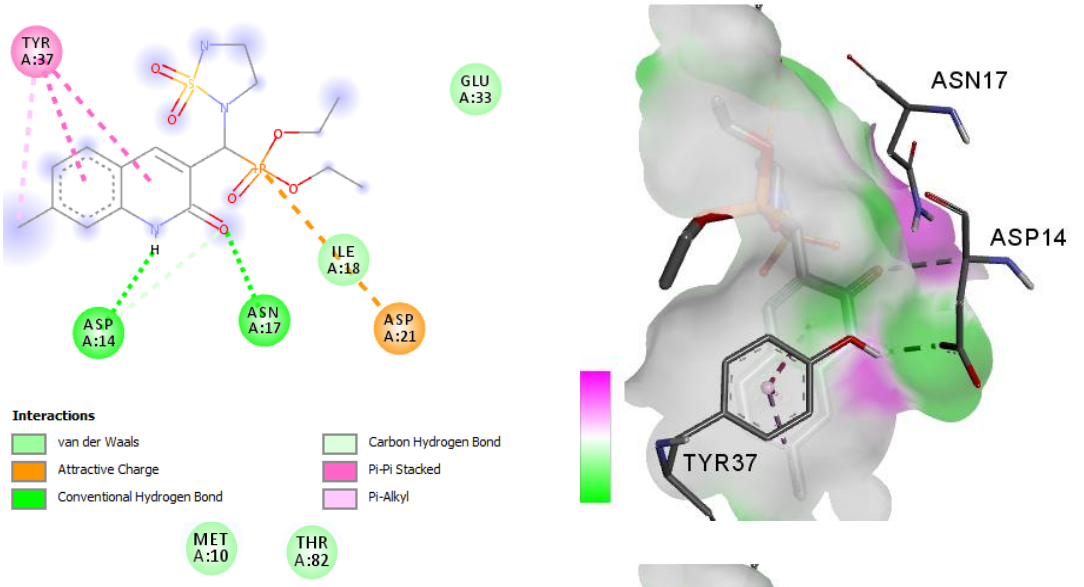

1XSD + Penicillin

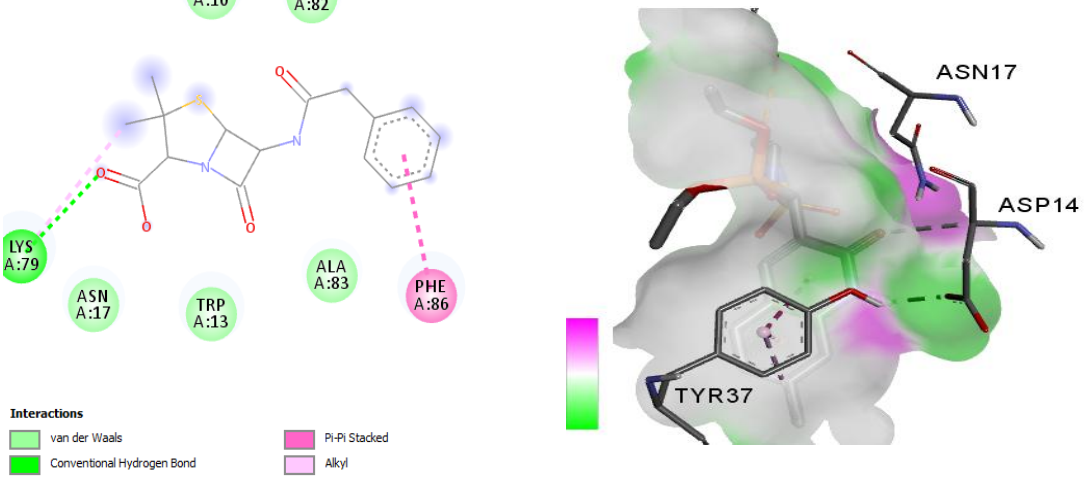

https://doi.org/10.26850/1678-4618.eq.v50.2025.e1594

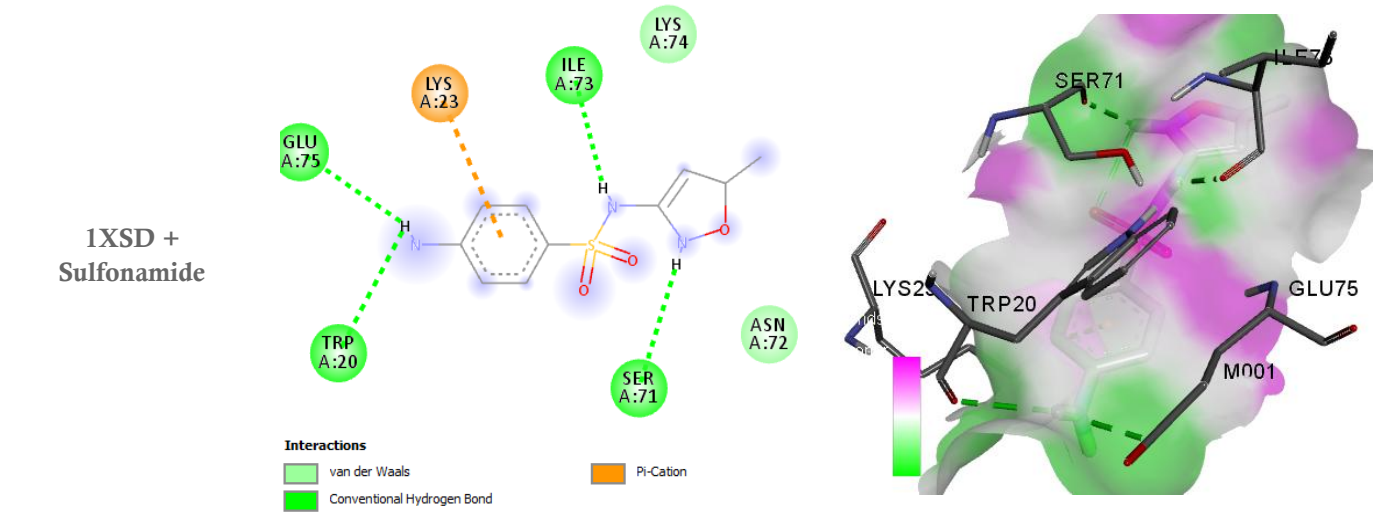

Figure 2. 2D and 3D of **1XSD** with the sulfamidophosphonates showing hydrogen interactions.
Source: Elaborated by the authors.

The calculated binding affinities for the ligands with **4WK3** receptor showed that the drugs interacted with **4WK3,** the bacterial secondary messenger involved in sensing integrity, cell wall metabolism and potassium transport. The binding affinities from the docking results showed that **NAK**, **NAN**, **5AD**, and **NAH** presented binding affinities of –23.0, –24.3, –25.1, and –25.5 kJ/mol, respectively. Additionally, NAL, NAJ, NAI, and NAM bind to 4wk3 receptors with affinities of –25.5, –25.9, –27.6, and –28.0 kJ/mol, respectively (**Table 2**). The H-bond formed between **4WK3** receptor amino acid residues and the drugs is within 3.5 Å. Other hydrophobic interactions of the medications with **4WK3** are displayed in **Fig. 3**. Compound **NAK** is H-bonded with LYS'29 and also has hydrophobic interactions with ALA'17, VAL'21, LYS'29 and THR'42; NAJ is hydrogen bonded with ASN'24, GLY'47, GLN'108, ARG'26, and formed hydrophobic interactions with ARG'26, GLN'108, GLY'47, VAL'48, ARG'26 and ARG'52; **NAN** showed H-bond interactions with ASP'10 THR'42 and **LYS'29**, hydrophobic interactions with SER'13 LYS'29 and THR'42; **5AD** is H-bonded with ARG'26 GLY'47 ARG'26 ASN'24 ARG'26 and ARG'52 and also has hydrophobic interactions with CYS'46 ARG'26 ARG'52, GLN'47 and ARG'26; **NAH** showed hydrophobic interactions with GLN'14 LYS'29 SER'13 and THR'42; **NAL** ARG'26 MET'1 PHE'106 GLN'108 GLY'47 ASN'49 and VAL'48; **NAI** showed hydrophobic interactions with THR'42 GLN'14 SER'13 and LYS'29; **NAM** showed hydrophobic interactions with VAL'103 PHE'106 THR'28 GLY'47 and ARG'26; whereas Penicillin is H-bonded to ASN'61 ASN'66 and ALA'96, and hydrophobically interacted with ASN'61 ASN'66 and ALA'96 residues (**Fig. 4**). Although no direct relationship is observed between the frontier energies of the ligands and the binding affinities, those ligands with higher IP presented good binding affinities. The results revealed that compounds NAH, NAL, NAN, NAI, NAJ, 5AD and NAM exhibited significant inhibitions against **4WK3** when compared with the standard drug (penicillin).

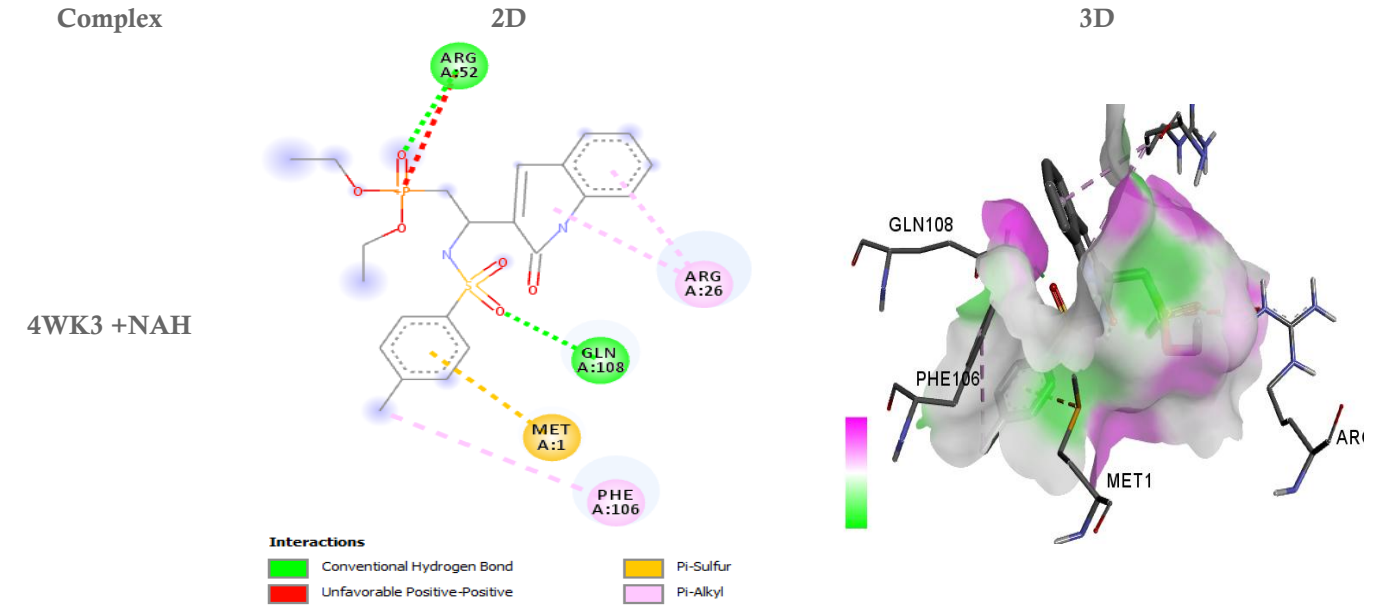

https://doi.org/10.26850/1678-4618.eq.v50.2025.e1594

4WK3 +NAI

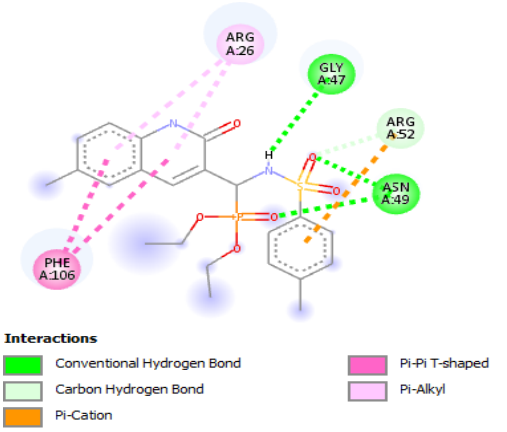

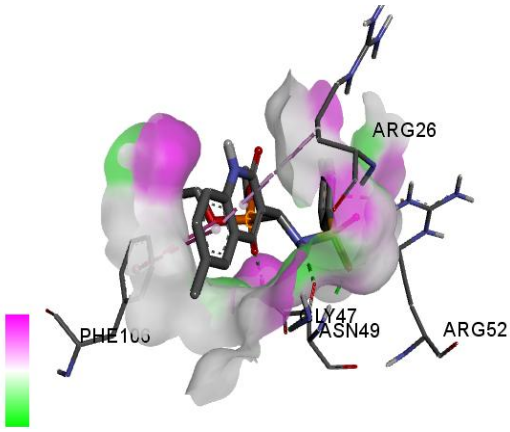

4WK3 +NAJ

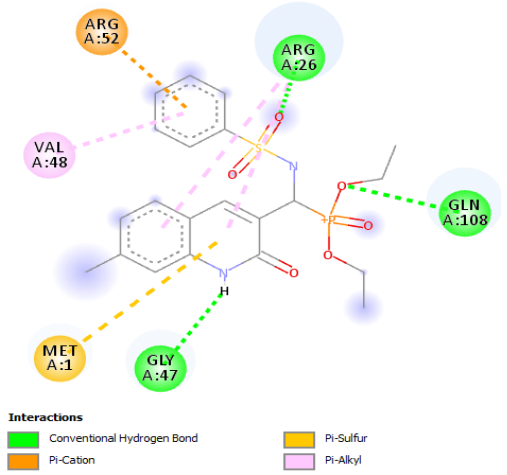

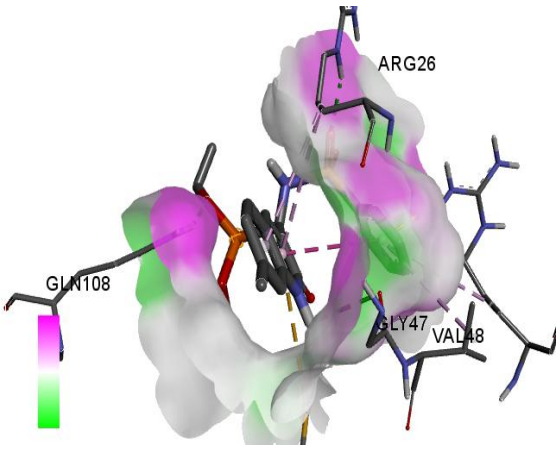

4WK3 +NAK

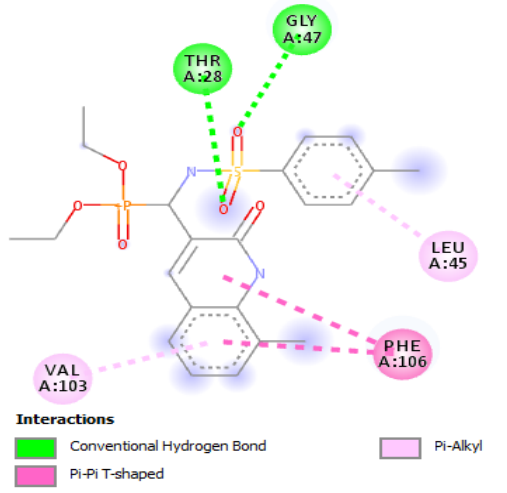

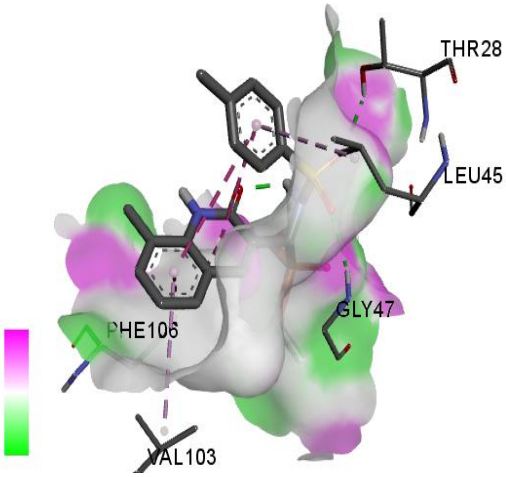

4WK3 +NAL

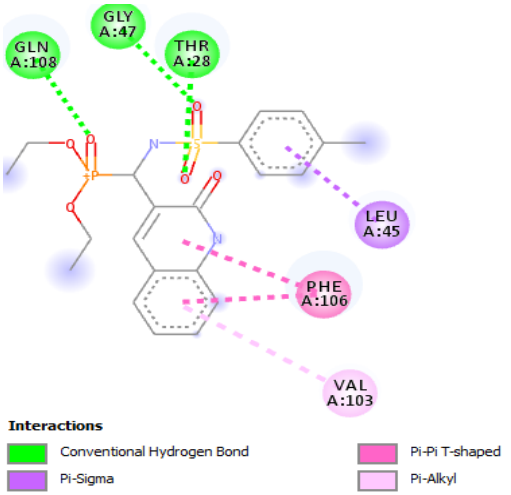

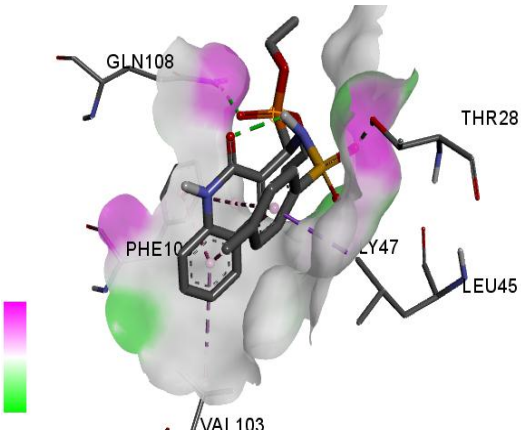

https://doi.org/10.26850/1678-4618.eq.v50.2025.e1594

4WK3 +NAM

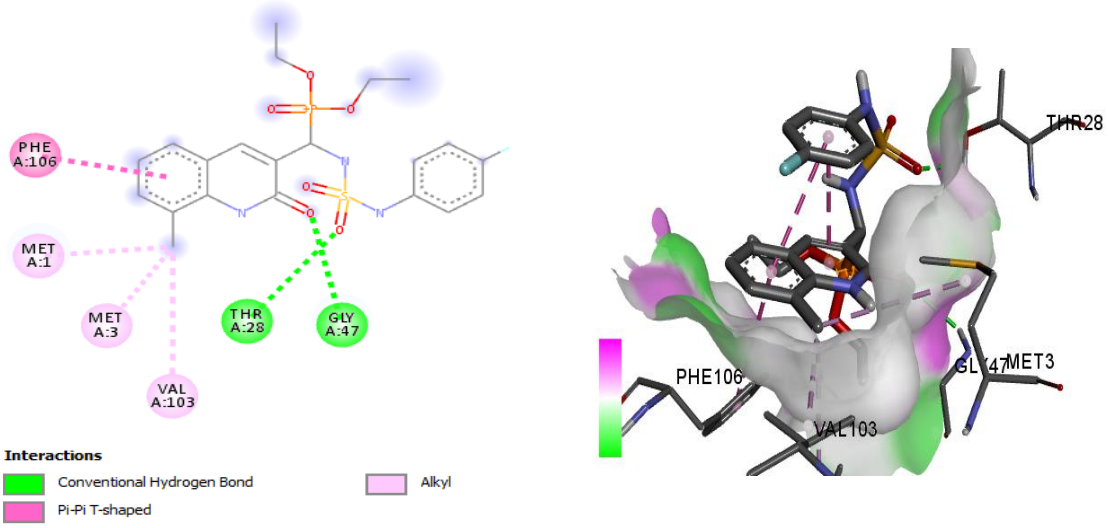

4WK3 +NAN

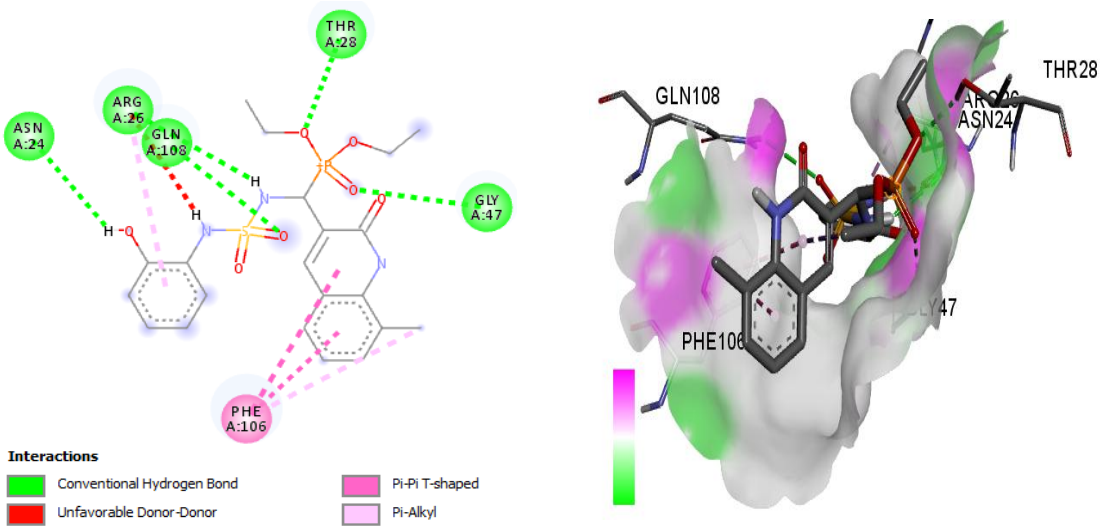

4WK3 +5AD

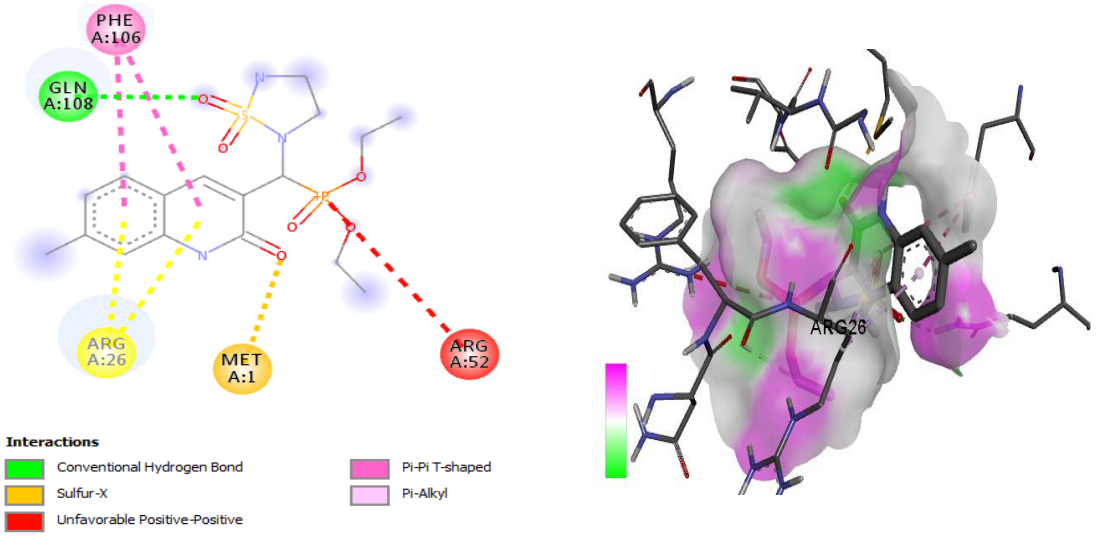

https://doi.org/10.26850/1678-4618.eq.v50.2025.e1594

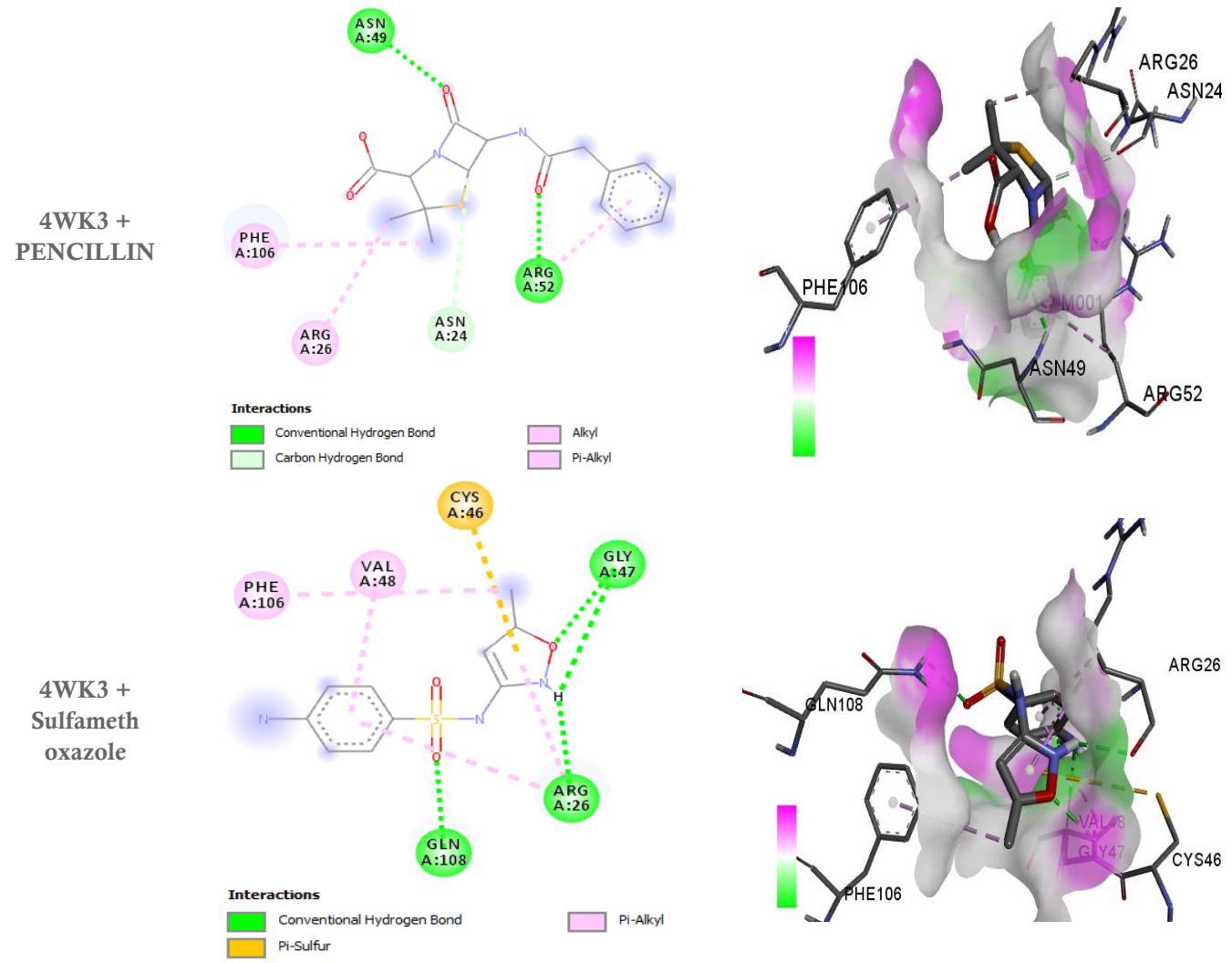

Figure 3. 2D and 3D of **4WK3** with sulfamidophosphonates showing hydrogen interactions.
Source: Elaborated by the authors.

3.3. Molecular dynamics simulation

In this study, the root mean square deviation (RMSD), root mean square fluctuation (RMSF), and actual binding energies for NAJ, NAN, and NAM, as well as the studied drug (Penicillin), were investigated and reported. As shown in **Table 3**, it was observed that NAJ proved to have the highest strength in inhibiting BlaI repressor (**1XSD**) than the studied reference compound. Additionally, the report in **Table 3** revealed that NAM has the lowest inhibitory activity compared to NAN and the reference compounds. More so, NAN with 2.3 kJ/mol as binding energy is expected to have the highest capacity to inhibit *Staphyloccus aureus* PstA (**PDB ID: 4WK3**) than NAM and the reference compound. In this work, the RMSD for NAJ-1XSD and NAN-4WK3 is presented in **Figs. 4** and **5**. As shown in the exact figures, the extent of deviation of the studied complex from its initial configuration bound to the studied receptor was examined in the calculated RMSD. The simulated system proved stable in the last five ps for the two selected compounds in **Table 3**.

Table 3. Calculated binding Energies for NAJ-1XSD, **NAM-4WK3** and **NAN-4WK3** with Penicillin-receptor complexes.

Complexes	Binding Energy Components (kJ/mol)				
	ΔE_{vdw}	ΔE_{ele}	ΔG_{gas}	ΔG_{sol}	ΔG_{bind}
NAJ-1XSD	−2.6±0.4	8±1	5±1	1.00±0.04	6.0 ± 1
Penicillin-1XSD	−29±2	−32±8	−61±6	79±9	18±3
NAM-4WK3	−2.2±0.5	−0.38±0.08	−0.38±0.08	3.5±0.3	3.1±0.4
NAN-4WK3	−2.1±0.4	0.1±0.1	1.0 ± 0.1	0.9±0.3	2.3±0.3
Penicillin-4WK3	−2.0±0.4	−0.3±0.2	−0.3±0.2	3±5	2.3±0.3

Source: Elaborated by the authors.

https://doi.org/10.26850/1678-4618.eq.v50.2025.e1594

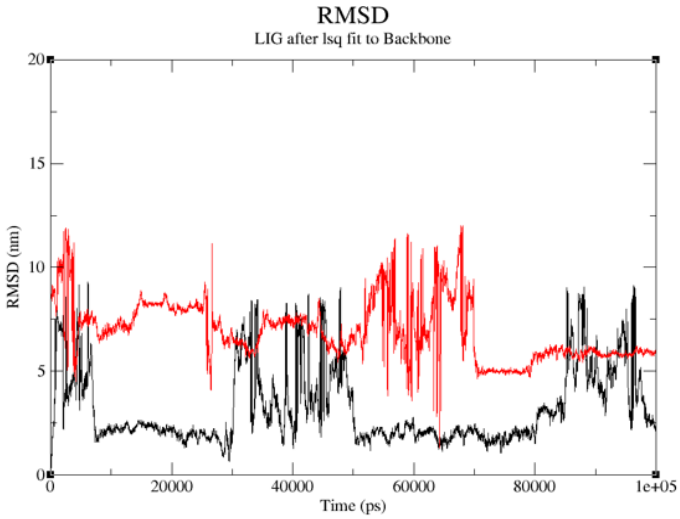

Figure 4. RMSD for **NAJ-1XSD** and **Penicillin-1XSD** complexes.
Source: Elaborated by the authors.

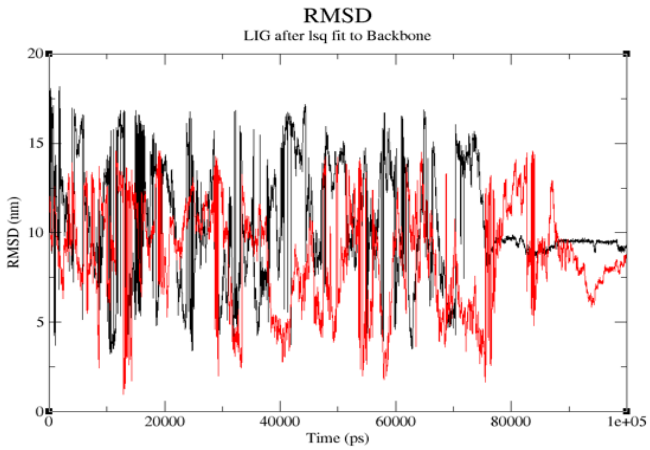

Figure 5. RMSD for **NAN-4WK3** and **Penicillin-4WK3** complexes.
Source: Elaborated by the authors.

3.3. ADME/pharmacokinetic predictions

Safety is paramount in drug usage; in this research, the physicochemical and ADMET properties of the ligands were assessed. However, there are lots of drug candidates that are not drug-like. Lipinski's rule of five (Ro5) was used to access the physicochemical properties of the ligands, which include molecular weight (150 ≤ MW ≤ 500), lipophilicity (log P ≤ 5), number of rotatable bonds (ROTBs ≤ 10), hydrogen bond donor (HBD ≤ 5) and hydrogen bond acceptor (HBA ≤ 10) (Daina *et al.*, 2017; Lipinski *et al.*, 2004). All the compounds and the standard drugs obeyed Lipinski's rule for hydrogen bond donors, hydrogen bond acceptors and molecular weight and WLogP. They are moderately soluble in water, whereas standard medicines are highly soluble. However, all the ligands have TPSA values between 132.75 and 165.01 Å, which are higher than 131.6 Å as the upper limit (**Table 4**).

Lack of efficacy and safety are the two major causes leading to drug failure (Sun *et al.*, 2022), which means the absorption, distribution, metabolism, excretion, and toxicity (ADMET) properties of chemicals play vital roles in every stage of drug discovery and development. *Hence, using ADMET profiling is considered* one way to reduce likely challenges associated with clinical trial treatments (Daina and Zoete, 2016; Darvas *et al.,* 2002). Compounds NAH, NAI, NAJ, NAK, NAL, NAM, NAN and 5AD were inhibitors to CYP3A4; therefore, they may cause an elevation in the concentration of the corresponding compounds, leading to drug overdose (Conrad *et al.*, 2024). Additionally, all the compounds except compound NAN exhibit high GI absorption, and none of the compounds possess blood–brain barrier BBB penetration. NAC, NAD, NAE, NAG, NAN, NAF, NAK, NAI, and NAM were identified as Pgp substrates (i.e. they can be transported out of the cell. Additionally, compounds NAD, NAE, and NAF could be inhibitors of Cyp2C19, while compounds NAC, NAG, NAN, NAK, 5AC and NAM could be substrates for Cyp2C19. None of the compounds could be inhibitor of Cyp2C9, and NAC was an inhibitor of Cyp2D6 (**Table 5**). The ADMET results revealed that NAF, NAI, NAK NAN and 5AC have attractive pharmacokinetic properties (**Table 5**).

Table 4. Physicochemical properties of sulfamidophosphonates.

Drugs	Mw g/mol	Heavy Atoms	Aromatic Heavy Atoms	Fraction Csp3	Rotatable Bonds	HBA	HBD	Molar Ref	TPSA	Lipinski violation	Log P (o/w)	Bio Score	H_2O solubility
NAH	478.50	32	16	0.32	10	7	2	124.79	132.75	0	3.03	0.55	Mod soluble
NAI	478.50	32	16	0.32	9	7	2	124.94	132.75	0	3.29	0.55	Mod soluble
NAJ	464.47	31	16	0.29	9	7	2	119.98	132.75	0	2.94	0.55	Mod soluble
NAK	478.5	32	16	0.32	9	7	2	124.94	132.75	0	3.33	0.55	Mod soluble
NAL	478.48	32	16	0.24	9	6	3	126.71	146.72	0	2.84	0.55	Mod soluble
NAM	497.48	33	16	0.29	10	8	3	125.11	144.78	0	3.23	0.55	Mod soluble
NAN	495.49	33	16	0.29	10	8	4	127.18	165.01	0		0.55	Mod soluble
5AD	429.43	28	10	0.47	7	8	2	114.55	135.96	0	1.49	0.55	Soluble
Penicillin	334.39	23	6	0.44	5	4	2	90.54	121.13	0	1.39	0.55	Soluble
Sulfameth-oxazole	253.28	17	11	0.1	3	4	2	62.99	106.6	0	-0.15	0.55	Soluble

Source: Elaborated by the authors.

Table 5. Pharmacokinetics properties of sulfamidophosphonates.

Drugs	GI Absorption	BBB Permeant	p-gp Substrate	CYP1A2 Inhibitor	CYP2C19 Inhibitor	CYP2C9 Inhibitor	CYP2D6 Inhibitor	CYP3A4 Inhibitor	Log K_p (skin Permeation) cm/s
NAH	Low	No	Yes	No	Yes	Yes	No	Yes	−7.28
NAI	Low	No	No	No	Yes	Yes	No	Yes	−6.95
NAJ	Low	No	No	No	Yes	Yes	No	Yes	−7.12
NAK	Low	No	No	No	Yes	Yes	No	Yes	−6.95
NAL	Low	No	Yes	No	No	No	No	Yes	−7.25
NAM	Low	No	Yes	Yes	No	No	No	Yes	−7.45
NAN	Low	No	Yes	No	No	No	No	Yes	−7.76
5AD	High	No	Yes	No	No	No	No	No	−8.63
Penicillin	High	No	No	No	No	No	No	No	−6.75
Sulfameth oxazole	High	No	No	No	No	No	No	No	−6.93

Source: Elaborated by the authors.

4. Conclusions

This study emphasized an *in-silico* assessment of anti-bacterial activities of sulfamidophosponate derivatives as compared with standard drugs (Penicillin and Sulfamethoxazole) against target proteins of *Staphylococcus aureus* via molecular docking and ADMET prediction. In this study, compounds NAH, NAL, NAI and NAJ exhibited stronger affinities than the standard (penicillin) against BlaI repressor in complex with DNA (PDB ID: **1XSD**), suggesting a better inhibitory potential than the standard drug. Furthermore, compounds NAH, NAI, NAJ, NAL, NAM, NAN and 5AD potentially inhibit **4WK3** than the standard drug (penicillin). These compounds could be inhibitors with potential for treating bacterial infection. Additionally, the ADMET results revealed that compounds NAG, NAE, NAH, and NAK have attractive pharmacokinetic properties. In general, this study demonstrated that compounds NAF, NAI, NAK and NAN could be potential inhibitors against *Staphylococcus aureus,* and they possess good pharmacokinetic properties, which are probable for drug discovery.

Authors' contribution

Conceptualization: Abimbola Modupe Olatunde, Kehinde Gabriel Obiyenwa; **Data curation**: Nathaniel Oladoye Olatunji; Kehinde Gabriel Obiyenwa; **Formal Analysis**: Nathaniel Oladoye Olatunji; Kehinde Gabriel Obiyenwa; **Funding acquisition**: Abimbola Modupe Olatunde, Kehinde Gabriel Obiyenwa; **Investigation**: Tofunmi Emmanuel Oladuji, Dayo Felix Latona; **Methodology**: Abimbola Modupe Olatunde, Kehinde Gabriel Obiyenwa; **Project administration**: Abel Kolawole Oyebamiji; Banjo Semire; **Resources**: Tofunmi Emmanuel Oladuji, Dayo Felix Latona; **Software**: Abel Kolawole Oyebamiji; Banjo Semire; **Supervision**: Abel Kolawole Oyebamiji; Banjo Semire; **Validation**: Tofunmi Emmanuel Oladuji, Dayo Felix Latona; **Visualization**: Abel Kolawole Oyebamiji; Banjo Semire; **Writing – original draft**: Abel Kolawole Oyebamiji; Banjo Semire; **Writing – review & editing**: Abel Kolawole Oyebamiji; Banjo Semire.

Data availability statement

All data sets were generated or analyzed in the current study.

Funding

Not applicable.

Acknowledgments

Not applicable.

Conflict of interest

The authors declare that there is no conflict of interest.

References

Adegbola, A. E.; Fadahunsi, O. S.; Alausa, A.; Abijo, A. Z.; Balogun, T. A.; Aderibigbe, T. S.; Semire, B.; Adegbola, P. I. Computational prediction of nimbanal as potential antagonist of respiratory syndrome coronavirus. *Inform. Med. Unlocked.* **2021a**, *24*, 100617. https://doi.org/10.1016/j.imu.2021.100617

Adegbola, P. I.; Semire, B.; Fadahunsi, O. S.; Adegoke, A. E. Molecular docking and ADMET studies of Allium cepa, Azadirachta indica and Xylopia aethiopica isolates as potential anti-viral drugs for Covid-19. *Virus Dis.* **2021b,** *32*, 85-97. https://doi.org/10.1007/s13337-021-00682-7

Adepoju A. J.; Latona D. F.; Oluwafemi Gbenga Olafare O. G.; Oyebamiji A. K.; Misbaudeen Abdul-Hammed M.; Semire B. Molecular docking and pharmacokinetics studies of Curcuma longa (Curcumin) potency against Ebola virus. *Ovidius University Annals of Chemistry.* **2022**, *33* (1), 23–35. https://doi.org/10.2478/auoc-2022-0004

Arora P.; Arora V.; Lamba H.; Wadhwa, D. Importance of Heterocylic Chemistry:A review. *International Journal of Pharmaceutical Science.* **2012**, *3* (9), 2947–2954.

Asibor, Y. E.; Oyebamiji, A. K.; Latona, D. F.; Semire, B. Computational screening of phytochemicals present in some Nigerian medicinal plants against sickle cell disease. *Scientific Reports.* **2024**, *14* (1), 26368. https://doi.org/10.1038/s41598-024-75078-w

Bazine, I.; Bendjedid, S.; Boukhari, A. Potential antibacterial and antifungal activities of novel sulfamidophosphonate derivatives bearing the quinoline or quinolone moiety. *Arch Pharm.* **2020**, *354*, e2000291. https://doi.org/10.1002/ardp.202000291

Bazine, I.; Cheraiet, Z.; Bensegueni, R.; Bensouici, C.; Boukhari A. Antioxidant and anticholinesterase activities of novel quinoline-aminophosphonate derivatives. *Journal of Heterocyclic Chemistry.* **2020**, *57* (5), 2139–2149. https://doi.org/10.1002/jhet.3933

Becke, A. Density functional thermochemistry. III. The role of exact exchange. *Journal of Physical Chemistry.* **1993**, *98* (7), 5648–5652. https://doi.org/10.1063/1.464913

Conrad, J.; Paras, N. A.; Vaz, R. J. Model of P-Glycoprotein Ligand Binding and Validation with efflux substrate Matched Pairs. *Journal of Medicinal Chemistry.* **2024**, *67* (7), 5854–5865. https://doi.org/10.1021/acs.jmedchem.4c00139

Daina, A.; Zoete, V. ABOILED-Egg to predict gastrointestinal absorption and brain penetration of small molecules. *Chem. Med. Chem.* **2016**, *11* (11), 1117–1221. https://doi.org/10.1002/cmdc.201600182

Daina, A.; Michielin, O.; Zoete, V. SwissADME: a free web tool to evaluate pharmacokinetics, drug likeness and medicinal chemistry friendliness of small molecules. *Scientific Reports.* **2017**, *7*, 1−13. https://doi.org/10.1038/srep42717

Darvas, F.; Keseru, G.; Papp, A.; Dorma´n, G.; Urge, L.; Krajcsi, P. In Silico and ex silico ADME Approaches for drug discovery. *Topics in Medicinal Chemistry*. **2002**, *2*, 1287–1304. https://doi.org/10.2174/1568026023392841

Farhan, A. K.; Sidra, M.; Sadia, N.; Umar, F.; Asma, Z.; Syed Majid, B.; Abdur, R.; Mohammad, S. M. Sulfonamides as potential bioactive scaffolds. *Curr. Org. Chem*. **2018**, *22*, 818−830. https://doi.org/10.2174/1385272822666180122153839

Flores-Holguín, N.; Frau, J.; Glossman-Mitnik, D. Calculation of the Global and Local Conceptual DFT Indices for the Prediction of the Chemical Reactivity Properties of Papuamides A-F Marine Drugs. *Molecules.* **2019**, *24* (18), 3312. https://doi.org/10.3390/molecules24183312

Forgacs, P.; Wengenack, N. L.; Hall, L.; Zimmerman, S. K.; Silverman, M. L.; Roberts, G. D. Tuberculosis and Trimethoprim-Sulfamethoxazole. *Antimicrobial Agents Chemotherapy*. **2009**, *53*, 4789–4793. https://doi.org/10.1128/AAC.01658-08

Hu, L.; Li, Z.-R.; Jiang, J.-D.; Boykin, D. W. Novel diaryl or heterocyclic sulfonamides as antimitotic agents. *Anti-Cancer Agents Med. Chem*. **2008**, *8* (7), 739−745. https://doi.org/10.2174/187152008785914806

Krátký, M.; Vinsová, J.; Volková, M.; Buchta, V.; Trejtnar, F.; Stolaríková, J. Antimicrobial activity of sulfonamides containing 5-chloro-2-hydroxybenzaldehyde and 5-chloro-2-hydroxybenzoic acid scaffold. *European Journal of Medicinal Chemistry*. **2012**, *50*, 433–440. https://doi.org/10.1016/j.ejmech.2012.01.060

Lee, C., Yang, W., and Parr, R. G., Development of the Colle-Salvetti correlation-energy formula into a functional of the electron density. *Phys. Rev. B* **1988,** 37, 785-789

Lipinski, C. A. Lead-and drug-like compounds: the rule-of-five revolution. *Drug Discovery Today: Technologies*. **2004**, *1* (4), 337–341. https://doi.org/10.1016/j.ddtec.2004.11.007

Manzanilla, B.; Robles, J. Conceptual DFT Reactivity Descriptors Computational Study of Graphene and Derivatives Flakes: Doped Graphene, Graphane, Fluorographene, Graphene Oxide, Graphyne, and Graphdiyne. *Journal of Mexican Chemical Society*. **2020**, *64* (3), 238–252. https://doi.org/10.29356/jmcs.v64i3.1167

Masters, P. A.; O'Bryan, T. A.; Zurlo, J.; Miller, D. Q.; Joshi, N. Trimethoprim-Sulfamethoxazole Revisited. *Archives of Internal Medicine.* **2003**, *163*, 402–410. https://doi.org/10.1001/archinte.163.4.402

Oyebamiji, A. K.; Fadare, O. A.; Akintelu, S. A.; Semire, B. Biological Studies on Anthra[1,9-cd]pyrazol-6(2D)-one Analogues as Anti-vascular Endothelial Growth Factor Via In silico Mechanisms. *Chemistry Africa*. **2021**, *4*, 955–963 https://doi.org/10.1007/s42250-021-00276-2

Oyebamiji, A. K.; Semire B. Dft-Qsar Model and Docking Studies of Antiliver Cancer (Hepg-2) Activities Of 1, 4-Diydropyridine Based Derivatives. *Cancer Biology.* **2016**, *6* (2), 69–72. https://doi.org/10.7537/marscbj06021610

Oyeneyin, O. E. DFT and Monte Carlo simulations on the corrosion inhibitive potentials of some furan-based carbohydrazide derivatives. *Letter of Applied NanoBio Science*. **2023**, *12* (4), 1–22. https://doi.org/10.33263/LIANBS124.113

Parr, R. G.; Szentpaly, L.; Liu, S. Electrophilicity index. *Journal of American Chemical Society*. **1999**, *121* (9), 1922–1924. https://doi.org/10.1021/ja983494x

Ramírez-Martínez, C.; Zárate-Hernández, L. A.; Camacho-Mendoza, R. L.; González-Montiel, S.; Meneses-Viveros, A.; Cruz-Borbolla, J. The use of global and local reactivity descriptors of conceptual DFT to describe toxicity of benzoic acid derivatives. *Computational and Theoretical Chemistry.* **2023**, *1226*, 114211. https://doi.org/10.1016/j.comptc.2023.114211

Rasigade, J. P.; Vandenesch, F. Staphylococcus aureus: a pathogen with still unresolved issues. *Infect. Genet. Evol*. **2014**, *21*, 510–514. https://doi.org/10.1016/j.meegid.2013.08.018

Ratchanok, P.; Prasit, M.; Veda, P.; Anusit, T.; Supaluk, P.; Somsak, R.; Virapong, P. Investigations on Anticancer and Antimalarial Activities of Indole Sulfonamide Derivatives and In Silico Studies. *ACS Omega.* **2021**, *6*, 31854−31868. https://doi.org/10.1021/acsomega.1c04552

Sun, D.; Gao, W.; Hu, H.; Zhou, S. Why 90% of clinical drug development fails and how to improve it? *Acta Pharmaceutica Sinica B*. **2022**, *12* (7), 3049–3062. https://doi.org/10.1016/j.apsb.2022.02.002

Supuran, C. T. Special Issue: Sulfonamides. *Molecules.* **2017**, *22* (10), 1642. https://doi.org/10.3390/molecules22101642

Thanikaivelan, P., Subramanian, V.; Rao, J. R.; Nair, B. U. Application of quantum chemical descriptor in quantitative structure activity and structure property relationship. *Chemical Physics Letter.* **2000**, *323* (1-2), 59–70. https://doi.org/10.1016/S0009-2614(00)00488-7

Trott, O.; Olson, A. J. AutoDock Vina: improving the speed and accuracy of docking with a new scoring function, efficient optimization and multithreading. *Journal of Computational Chemistry*. **2010**, *31*, 455–461. https://doi.org/10.1002/jcc.21334

Hehre, W. J.; Radom, L.; Schleyer, P. V. R.; Pope, J. A. *Ab initio molecular Orbital Theory*, Wiley, New York, 1988

Waring, M. J.; Arrowsmith, J.; Leach, A. R.; Leeson, P. D.; Mandrell, S.; Owen, R. M. An analysis of the attrition of drug candidates from four major pharmaceutical companies. *Nat. Rev. Drug. Discov*. **2015**, *14*, 475–486. https://doi.org/10.1038/nrd4609

Wertheim, H. F.; Melles, D. C.; Vos, M. C.; van Leeuwen, W.; van Belkum, A.; Verbrugh, H. A.; Nouwen, J. L. The role of nasal carriage in *Staphylococcus aureus* infections. *Lancet Infect Dis.* **2005**, *5* (12), 751–762. https://doi.org/10.1016/S1473-3099(05)70295-4

Winum, J. Y.; Scozzafava, A.; Montero, J. L.; Supuran, C. T. Therapeutic potential of sulfamides as enzyme inhibitors. *Med. Res. Rev*. **2006**, *26* (6), 767–792. https://doi.org/10.1002/med.20068

Yang, L.; Feng, J.; Ren, A. Theoretical studies on the electronic and optical properties of two thiophene–fluorene based π-conjugated copolymers. *Polymer.* **2005**, *46* (24), 10970–10982. https://doi.org/10.1016/j.polymer.2005.09.050

Zhao, C.; Rakesh, K. P.; Ravidar, L.; Fang, W. Y.; Qin, H. L. Pharmaceutical and medicinal significance of sulfur (SVI)-Containing motifs for drug discovery: A critical review. *Eur. J. Med. Chem*. **2019**, *162*, 679−734. https://doi.org/10.1016/j.ejmech.2018.11.017